Mn and Fe Modified Fly Ash As a Superior Catalyst for Elemental Mercury Capture under Air Conditions

ARTICLE *in* ENERGY & FUELS · JULY 2012

Impact Factor: 2.79 · DOI: 10.1021/ef3005256

3 AUTHORS, INCLUDING:

Lili Xing
Wuxi Center For Disease Control
2 PUBLICATIONS **21** CITATIONS
SEE PROFILE

Qin Zhong
128 PUBLICATIONS **776** CITATIONS
SEE PROFILE

energy&fuels

Article

pubs.acs.org/EF

Mn and Fe Modified Fly Ash As a Superior Catalyst for Elemental Mercury Capture under Air Conditions

Lili Xing, Yalin Xu, and Qin Zhong*

School of Chemical Engineering, Nanjing University of Science and Technology, Nanjing 210094, PR China

ABSTRACT: The objective of this study was to investigate the effects of fly ash (FA) and Mn and Fe modified FA on elemental mercury capture under air at 120 °C. X-ray fluorescence spectrometry (XRF), Brunauer−Emmett−Teller (BET) surface area, scanning electron micrographs (SEMs), X-ray diffraction (XRD), thermogravimetric (TG) analysis, and X-ray photoelectron spectroscopy (XPS) were employed to characterize the samples. The results showed that the cooperation of Mn and Fe loaded on FA improved the performance of elemental mercury capture in a laboratory packed-bed reactor. In the presence of O_2, Mn(2)−Fe(3)−FA (FA modified with an Mn/Fe molar ratio of 2/3) possessed the best reactivity and its Hg^0 removal efficiency stayed around 98% within 8 h. The heterogeneous mercury reaction could be speculated as: Hg^0 was physically adsorbed on the cation vacancies and then was oxidized to HgO by Mn^{4+} and Fe^{3+} cations. The reduced forms of Mn^{3+} and Fe^{2+} reoxidized under air, and HgO was finally adsorbed on the surface of the catalysts.

1. INTRODUCTION

The emission of mercury from anthropogenic activities has become a serious concern in both developed and developing countries.[1] In fact, coal-fired utility boilers are the largest anthropogenic source of Hg emission. In China, about 38% of mercury air emissions come from coal combustion.[2] Because of its toxicity, mobility, and bioaccumulation in the ecosystem and food chain, mercury has attracted more and more attention. In addition to particulate bound mercury (Hg^P), elemental mercury (Hg^0) and oxidized mercury (Hg^{2+}) are present as the gaseous mercury species in the flue gas from coal-fired utility boilers.[2] Hg^P and Hg^{2+} can be effectively removed by particulate control devices and wet scrubbing or SO_2 control devices, respectively.[3] However, Hg^0 is very hard to remove due to its high volatility and low solubility in water. Therefore, Hg^0 is the primary species of mercury emitted from industrial stacks.

Various methods, mainly including adsorption and catalytic-oxidation, have been proposed for the control of Hg^0 emissions and evaluated from bench to pilot scale in the past few decades.[4,5] Of these methods, the particulate adsorption method is the most common one. Activated carbon injection (ACI) into flue gas seems to be one of the simplest and best characterized approaches to control the mercury emissions from coal-fired boilers. To improve the effectiveness of Hg^0 capture, activated carbons have been chemically modified with oxidizers, such as Br,[6] Cl,[7] and sulfur-containing substances.[8,9] These studies present that chemically modified activated carbon (AC) may be more effective in Hg^0 removal. However, the operating cost of control of elemental mercury by ACI is estimated in the range of 0.14 to 3.92 mills kW h^{-1}, which limits the widespread use of this technique, especially in developing countries.[10] Furthermore, current research indicates that, compared with Br, Cl, sulfur, etc., catalytic oxidation of elemental mercury with gaseous oxygen as the oxidant in flue gas is an economical method for elemental mercury control.[11] In air conditions, the oxidized mercury (HgO or Hg_2O) is in a solid state below 300 °C, so it may be adsorbed by the catalyst and then removed from the flue gas.[12,13] Therefore, it is desirable to find an economical and environment-friendly method for elemental mercury control.

Since wide scale coal firing for power generation began in the 1920s, millions of tons of fly ash (FA) and related byproduct have been generated.[14] It is known that the utilization of FA is helpful for economic development and environmental protection. But the current utilization of FA worldwide accounts for only a small part of the total FA. Many studies have been conducted on the use of waste FA in the removal of various pollutants. It was found that when FA was used as an adsorbent for the capture of mercury, accompanying oxidation was observed,[15] and little mercury was released from FA even at 300 °C,[16] which revealed that the mercury captured on FA may be thermally stable.

Recently many materials, such as $MnCl_2$/AC, $CoCl_2$/AC, Mn^{x+}/ $Ca(OH)_2$, CeO_2/HZSM-5, and CeO_2/γ-Al_2O_3, have been used for the study of mercury removal.[17−20] However, FA and especially modified FA have seldom been reported in this respect. Over the past few years, Fe−Mn mixed oxides have attracted considerable attention due to their excellent performance as catalysts.[21] In Fe−Mn mixed oxides, iron cations are replaced by manganese cations and an equivalent number of cation vacancies are incorporated to maintain the spinel structure.[22] Hg^0 is a Lewis base because it can be an electron-pair donor. Cation vacancies on the surface are Lewis acid sites, which can provide the active sites for the physical adsorption of Hg^0.[10,11,23,24] Yang et al. found that under air conditions, Fe−Mn mixed oxides showed a promising application in the elemental mercury capture at low reaction temperature.[10,23,24]

Therefore, in this paper, Mn and Fe were loaded on FA, and experiments were carried out at 120 °C (near the temperature of a stack) in a packed-bed reactor system. The importance of

Received: March 30, 2012
Revised: July 12, 2012
Published: July 13, 2012

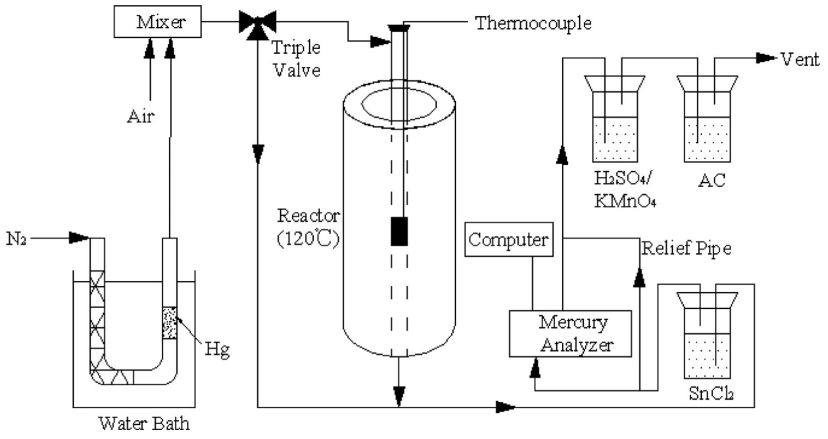

Figure 1. Schematic diagram of experimental system.

Table 1. Major Chemical Composition of Fly Ash (wt %)

SiO_2	Al_2O_3	CaO	Fe_2O_3	TiO_2	K_2O	MgO	SO_3	P_2O_5	SrO	ZrO_2	MnO	CuO	unburned carbon
55.10	27.84	3.56	4.76	0.95	1.83	1.11	0.77	0.20	0.072	0.020	0.068	0.010	3.24

O_2 for the capture of mercury was studied. The heterogeneous mercury reaction was speculated by thermogravimetric (TG) and X-ray photoelectron spectroscopy (XPS) analysis.

2. EXPERIMENTAL SECTION

2.1. Catalyst Preparation. The fly ash was collected from the hoppers of the ESP in the Flue Gas Purification Engineering, within the project of Technical Reform for Energy Conservation and Comprehensive Utilization of Shanxi Yanchang Petroleum Xinghua Chemical Co., Ltd. The coals burned were lignites. First, FA was washed with deionized water, and then dried in an electric blast drying oven at 120 °C for 24 h. After that, the sample was stored in a desiccator for future use. $Fe(NO_3)_3$ and $Mn(CH_3COOH)_3{\cdot}4H_2O$ were loaded on FA as follows: First, $Fe(NO_3)_3$ and $Mn(CH_3COOH)_3{\cdot}4H_2O$ were dissolved in deionized water to form the solution. Then, FA was added to the solution under a constant temperature and stirring in a proportion corresponding to the Fe and Mn loading values of 10 wt %. After 1 h, the samples were dried in an electric blast drying oven at 120 °C for 12 h. Then the dried samples of Mn(x)−Fe(y)−FA (with different Mn/Fe molar ratios of x/y) were calcined in a muffle furnace at 500 °C for 4 h and then cooled to ambient temperature. Finally, the samples were stored in a desiccator for future use. In this study, the weight percentage of the impregnated Fe and Mn to FA was set at 10% if it was not stated clearly.

2.2. Catalyst Characterization. X-ray fluorescence (XRF) spectrometry (ARL9800XP) was used to determine the chemical composition of FA (in weight percent). X-ray diffraction (XRD) patterns were recorded on a Beijing Purkinjie general instrument XD-3 X-ray diffraction (CuKα, voltage 35 kV, electrical current 20 mA, 2θ from 5° to 80°). Specific surface areas of the catalysts were determined by N_2 adsorption−desorption measurements at 77 K by employing the Brunauer−Emmet−Teller (BET) method (Gold App V-sorb 2008). Prior to N_2 adsorption, the sample was outgassed at 200 °C for 12 h to desorb moisture adsorbed on the surface and inside the porous network. Microstructures of the catalysts were observed by scanning electron micrograph (SEM) in JEOLJSM-6380LV (Japan) system at a voltage of 20 kV. X-ray photoelectron spectroscopy (XPS) experiments were carried out on a RBD upgraded PHI-5000C ESCA system (Perkin-Elmer). The thermogravimetric (TG) analysis of samples were performed with a Netzsch STA 449C Jupiter instrument. For each test, approximately 1.4 mg of sample was heated from 50 to 600 °C at the heating rate of 10 °C min^{-1} under nitrogen atmosphere (>99.99%).

2.3. Elemental Mercury Capture. Figure 1 shows a schematic diagram of the experimental system, which included four parts: an elemental mercury permeation tube, a packed-bed reactor, an online QM201H mercury analyzer and a tail-end absorption equipment. A flow of N_2 (200 mL/min) was used as Hg^0-laden gas stream by passing through the Hg^0 permeation tube. To guarantee a constant permeation concentration, the Hg^0 permeation tube was placed in a U-shaped glass tube, which was immersed in a constant temperature (50 °C) water bath. The gas containing elemental mercury first entered the QM201H to determine the inlet mercury concentration (20 ± 1 $\mu g/m^3$). The detection limit was 0.001 $\mu g/m^3$, and the nominal range was 0.01−100 $\mu g/m^3$. When the mercury analyzer had been stable for more than 30 min, the gas was diverted to the catalyst bed for the tests, and then the outlet Hg^0 concentration was measured. The Hg^0-laden stream was transferred throughout the system using Teflon tubing, which was heated to prevent condensation of Hg^0 and to preheat the gas to the reactor temperature. The exhaust gas from the mercury analyzer was introduced into $H_2SO_4/KMnO_4$ solution and activated carbon before being expelled into the atmosphere.

About 1 g of the catalyst was inserted in the middle of the quartz tube (i.d. 12 mm) and then packed with quartz wool to support the catalyst layer and avoid its loss. The catalysts were first tested under air to estimate the performance for elemental mercury capture. The total flow rate was maintained at 1 L/min (corresponding to a space velocity of about 53 000 h^{-1}), and then, the flow was matched into the mercury analyzer. The commercial QM201H mercury analyzer was essentially a portable cold vapor atomic absorption (CVAA) apparatus that was designed to measure only Hg^0. So the $SnCl_2$ impinger was used to reduce the oxidized mercury to elemental mercury. And then, the total amount of mercury in the sampled gas was detected. Therefore, the reduced amount of elemental mercury was captured by the catalysts. For the whole tests, the Hg removal efficiency (η) was defined as

$$\eta = \frac{Hg_{in} - Hg_{out}}{Hg_{in}} \times 100\% \quad (1)$$

where Hg_{in} and Hg_{out} are the Hg inlet and outlet concentrations, respectively.

The error of experiment was inevitable. Hence, the mercury removal points in the figures were the average of three experimental data. The results of the experiments showed good repetitiveness.

3. RESULTS AND DISCUSSION

3.1. Characteristics of the Sample. *3.1.1. XRF.* Table 1 showed that the primary chemical components in FA included SiO_2, Al_2O_3, CaO, Fe_2O_3, unburned carbon, K_2O, MgO, TiO_2, SO_3, and P_2O_5. As reported, when temperature was at or below

dx.doi.org/10.1021/ef3005256 | Energy Fuels 2012, 26, 4903−4909

150 °C, mercury could be oxidized by the oxide composition of fly ash particles.[16,25] CuO, Fe_2O_3, Al_2O_3, TiO_2, CaO, and unburned carbon in FA may act as catalysts for mercury oxidation,[26−28] which allowed FA to be suitable for the application in mercury capture.

3.1.2. BET. The porous structure parameters of samples are shown in Table 2. It could be observed that the raw FA had the lowest BET surface area and the smallest pore volume, 0.30 and 0.002 cm^3/g, respectively. When Fe was loaded on FA, the BET surface area and total pore volume were significantly increased. Meanwhile, the BET surface area increased with the participation of Mn, while they decreased with an increase in the Mn/Fe molar ratio of (2:3). The reason may be that the manganese oxides were impregnated on the surface of FA and blocked some pores.

Table 2. Porous Structure Parameters of the Samples

sample	BET surface area (m^2/g)	total pore volume (cm^3/g)
FA	0.30	0.002
Mn(0)−Fe(3)−FA	23.51	0.072
Mn(1)−Fe(3)−FA	24.47	0.050
Mn(2)−Fe(3)−FA	17.02	0.038
Mn(1)−Fe(0)−FA	7.30	0.027

3.1.3. SEM. The SEM pictures of raw FA and Mn(2)−Fe(3)−FA are shown in Figure 2. Figure 2a showed that most of the agglomerated particles with the uniform size in FA were well-rounded and spherical in shape, and only a few were irregular in shape. This was in line with other reports that FA particles from coal combustion were primarily spherical.[29,30] From the figures, it was observed that the surfaces of FA were relatively smooth. However, the surfaces of Mn(2)−Fe(3)−FA were rougher, which appeared spongy. It revealed that the external surfaces of these large spheres had plenty of Mn and Fe particles attached, which greatly enhanced the surface roughness of the FA particles.

3.1.4. XRD. XRD patterns of the catalysts are listed in Figure 3. This figure showed that the main phases present in raw FA

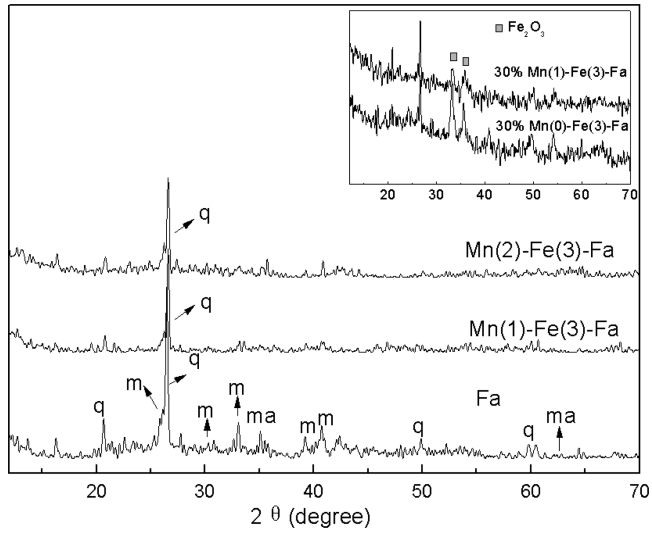

Figure 3. X-ray diffraction patterns of fly ash (m = mullite, q = quartz, ma = maghemite).

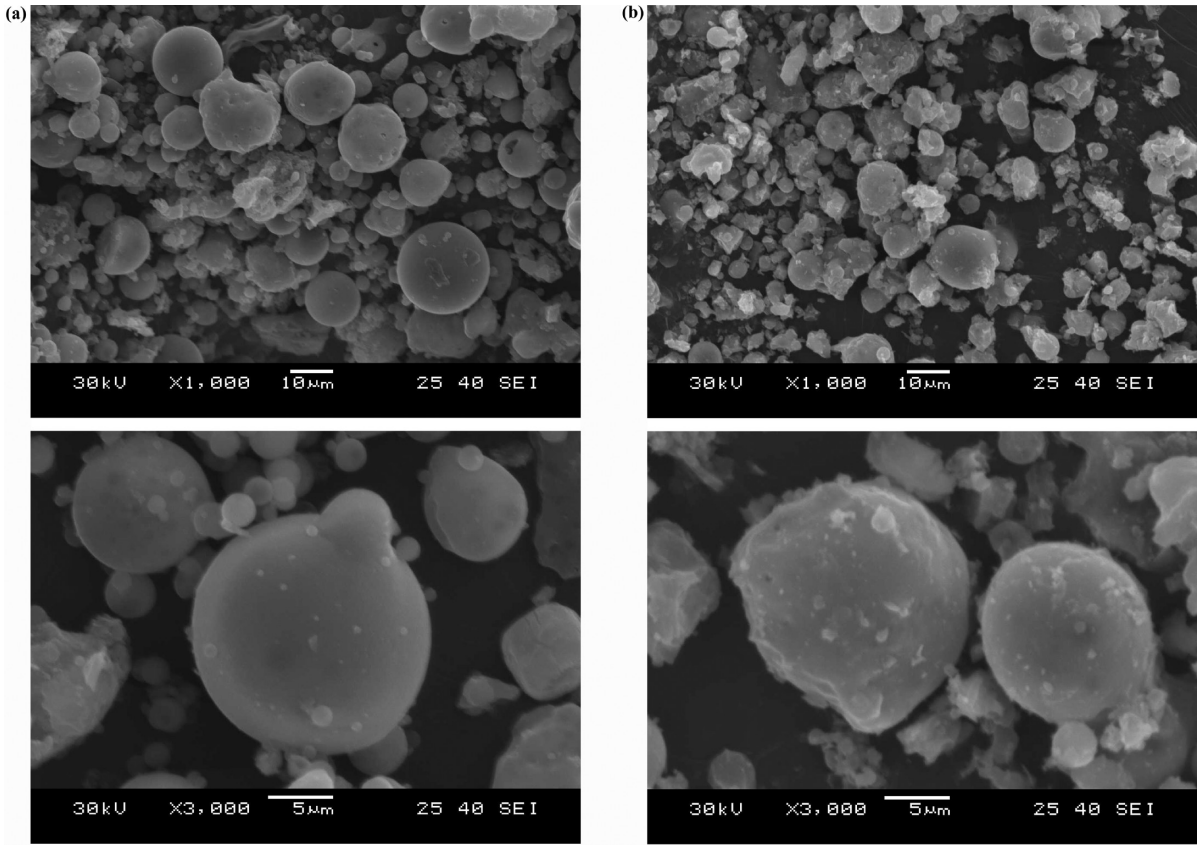

Figure 2. SEM photographs of (a) pure FA and (b) Mn(2)−Fe(3)−FA.

dx.doi.org/10.1021/ef3005256 | *Energy Fuels* 2012, 26, 4903−4909

were crystalline components, such as: quartz (SiO_2), mullite ($Al_6Si_2O_{13}$), and Tridymite-O (SiO_2), which were always present as the major phases in coal combustion fly ash.[29,31] In Mn and Fe doped FA samples, quartz, etc., was also the predominant form, and the intensity of peaks attributed to quartz decreased, suggesting that Mn and Fe interacted with these crystalline components in the catalysts. The reason for no peaks for the doped metals on the catalysts was likely due to the small amount of them below the detection limit of XRD. However, when the loading value was increased to 30%, it could be seen that Fe mainly was presented in the form of Fe_2O_3, but the peak for Mn oxides still could not be observed. From the figure, the full width at half-maximum (fwhm) of Fe_2O_3 peaks was slightly increased after the FA was doped with Mn. The higher XRD fwhm of the crystalline indicated the smaller size of the particles, which showed that Mn could improve the dispersion of Fe_2O_3 particles by inhibiting the agglomeration. It agreed well with the results that the BET surface area of Mn(1)−Fe(3)−FA was larger than that of Mn(0)−Fe(3)−FA.

3.2. Performance for Elemental Mercury Capture in Air. Figure 4 shows the removal efficiency of elemental

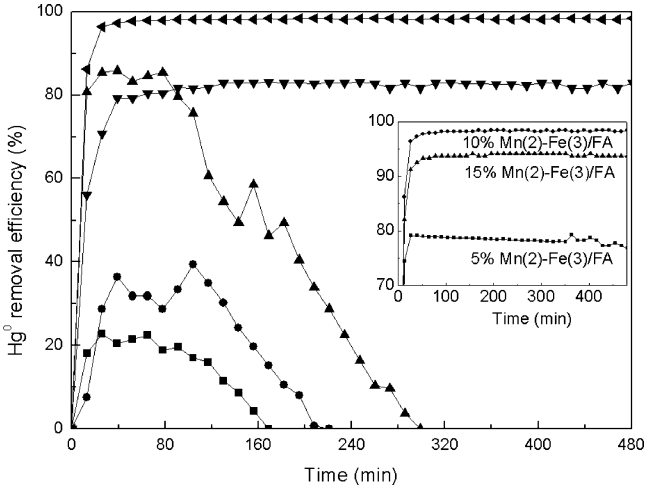

Figure 4. Removal efficiency of elemental mercury capture by FA and modified FA under air: ■, FA; ●, Mn(0)−Fe(3)−FA; ▲, Mn(1)−Fe(0)−FA; ▼, Mn(1)−Fe(3)−FA; ◀, Mn(2)−Fe(3)−FA.

mercury capture by FA and modified FA under air conditions. The most active sample was found with 10% Fe and Mn content. FA did have the capacity for the mercury capture, but there was no adsorption capacity after 160 min. The performance of the modified FA was also investigated to obtain a satisfactory result. On one hand, when not loaded with Mn, Mn(0)−Fe(3)−FA showed a slightly higher Hg^0 removal ability than FA: the efficiency of Mn(0)−Fe(3)−FA was about 38%, and the efficiency of FA was nearly 20%. Apparently, the doped Fe had a slight influence on the Hg^0 removal efficiency. On the other hand, when not loaded with Fe, the efficiency of Mn(1)−Fe(0)−FA reached about 85%, which was better than that of Mn(1)−Fe(3)−FA within about half an hour. It was disappointing that the waning chemical adsorption led to the decrease of removal efficiency, and Mn(1)−Fe(0)−FA was finally saturated. However, it was remarkable that the activity of Mn(1)−Fe(3)−FA showed good stability and showed Hg^0 removal efficiency around 82% with 8 h. When the Mn/Fe molar ratio was increased, Mn(2)−Fe(3)−FA provided more excellent Hg^0 removal efficiency around 98%. In this study, catalysts with other higher Mn/Fe molar ratio were also investigated, the efficiency was similar to that of Mn(2)−Fe(3)−FA. Therefore, Mn(2)−Fe(3)−FA was one of the most suitable catalysts for the mercury capture. The total experimental results indicated that the cooperation of Mn and Fe had obvious accelerative effects on Hg^0 removal, and Mn may be the main active site.

Figure 5 showed that elemental mercury capture by Mn(2)−Fe(3)−FA in air was much better than that in N_2. Unlike the

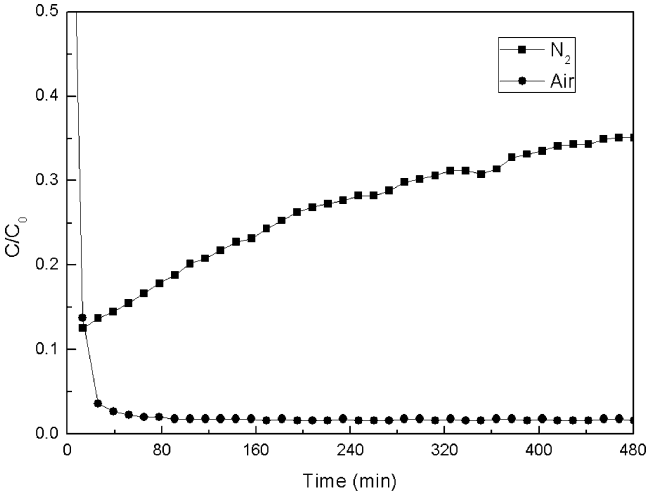

Figure 5. Breakthrough curves of elemental mercury capture by Mn(2)−Fe(3)−FA under air and N_2.

experiments with N_2, when Mn(2)−Fe(3)−FA was in air, the removal efficiency remained constantly at about 98% for the entire 8 h. This indicated that the presence of O_2 may be helpful for the regeneration of Mn(2)−Fe(3)−FA. In this case, Mn(2)−Fe(3)−FA was likely to be a catalyst, rather than an adsorbent.

3.3. Speculation on the Heterogeneous Mercury Reaction for the Modified FA. *3.3.1. TG Analysis.* To determine the speciation of mercury on the used Mn(2)−Fe(3)−FA, TG was performed. As shown in Figure 6, there was a quick initial mass loss as temperature increased up to 100 °C,

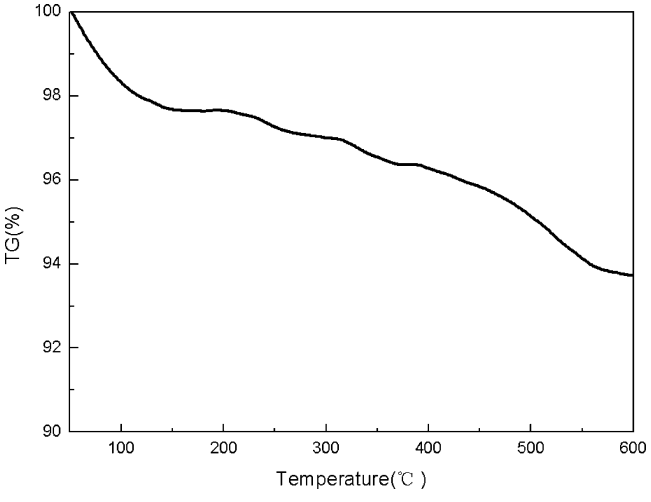

Figure 6. TG analyses of the used Mn(2)−Fe(3)−FA.

dx.doi.org/10.1021/ef3005256 | Energy Fuels 2012, 26, 4903−4909

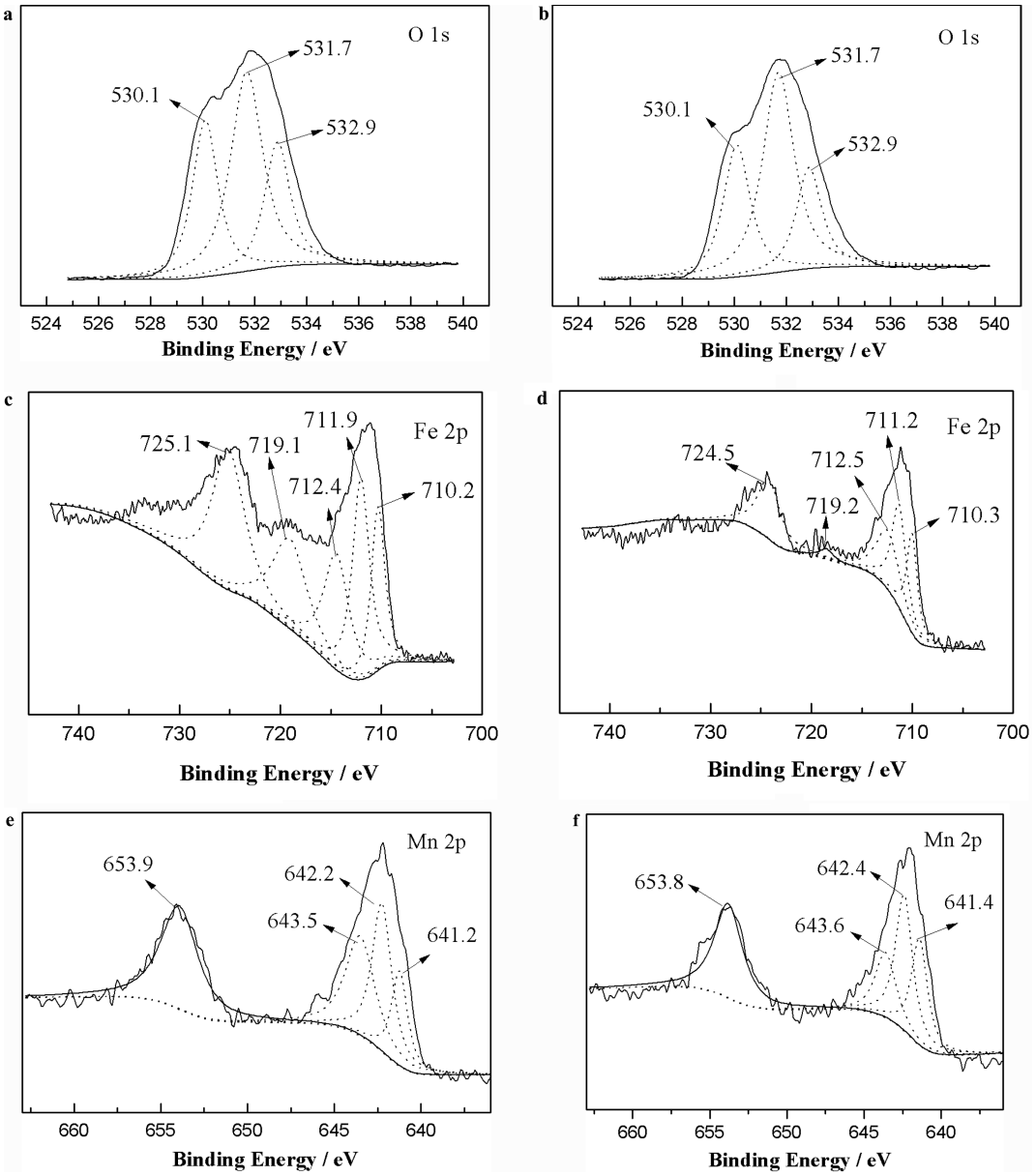

Figure 7. XPS spectra of the samples over the spectral regions of Mn 2p, Fe 2p, and O 1s.

which corresponded to the loss of desorbed water. At 100 °C, the rate of mass loss changed and weight loss occurred much more slowly. At this point, Hg^0 was evaporating, and this was a slow process because the boiling point of mercury was 357 °C and the mass of adsorbed Hg^0 on the catalyst was smaller than the mass of water.[32] The weight loss between 400 and 500 °C was attributed to HgO.[20,32,33] Furthermore, the weight loss may occur at temperatures higher than 500 °C because the pores of the catalyst increased the boiling point of HgO and also caused Hg^0 to evaporate more slowly.[33]

3.3.2. XPS Analysis. Surface information on synthesized samples was analyzed by XPS. XPS spectra over the spectral regions of O 1s, Fe 2p, and Mn 2p were evaluated. The O 1s peak centered at about 530.1 eV, as expected for the transition metal oxides. Other oxygen species at about 531.7 eV was also observed in the XPS spectra, which was assigned to −OH. Furthermore, a peak at about 532.9 eV was ascribed to the adsorbed H_2O. In comparison with fresh Mn(2)−Fe(3)−FA (shown in Figure 7a), no obvious changes happened in the XPS spectra over the spectral regions of O 1s after elemental mercury capture (shown in Figure 7b).

The peaks of Fe species on fresh Mn(2)−Fe(3)−FA were assigned to oxidized Fe species, more likely Fe^{3+} type species.[34,35] The binding energies centered at about 710.2, 711.9, and 712.4 eV may be assigned to Fe^{3+} cations (shown in Figure 7c). The peak at about 719.1 eV was the fingerprint of the Fe^{3+} species, which indicated that all iron ions on the surface of the catalysts may be exclusively in Fe^{3+} state.[36] However, it could not be firmly stated that other iron species were absent. The presence of oxidized iron species alone may be due to a surface oxidation process before the analysis as already reported.[37] After elemental mercury capture, no obvious changes of valence happened. The binding energies centered at about 710.3, 711.2, and 712.5 eV were all the fingerprint of the Fe^{3+} species (shown in Figure 7d).[11,23]

The Mn peaks at 641.2 and 642.2 eV were assigned to Mn^{3+} and Mn^{4+}, respectively (shown in Figure 7e).[11] After elemental mercury capture, the Mn peaks were assigned to Mn^{3+} (641.4

dx.doi.org/10.1021/ef3005256 | *Energy Fuels* 2012, 26, 4903−4909

eV) and Mn^{4+} (642.4 eV) (shown in Figure 7f). Meanwhile, in comparison with fresh Mn(2)−Fe(3)−FA, the ratio of Mn^{4+} cation to Mn^{3+} cation was decreased from 1.91 to 1.34 (shown in Table 3), which was in line with previous reports that some

Table 3. XPS Results of Mn(2)−Fe(3)−FA before and after Elemental Mercury Capture

	surface atomic concentration (%)		
	Mn		surface atomic ratio
samples	Mn^{3+}	Mn^{4+}	Mn^{4+}/Mn^{3+}
before	1.43	2.72	1.91
after	1.72	2.31	1.34

Mn^{4+} cations were reduced to Mn^{3+} cations during elemental mercury capture.[10,11,23,24] Furthermore, previous research demonstrated that during the interactions between Mn oxide and ferrites, an equivalent number of cation vacancies would be incorporated to the surface of catalysts.[10,11,24,38] As a Lewis base, elemental mercury was physically adsorbed on the cation vacancies (≡•, Lewis acid sites), and then could be oxidized by Mn^{4+} cations.[10,11,23,24] Although the BET surface area of Mn(2)−Fe(3)−FA decreased after adding more Mn, the concentrations of Mn^{4+} and cation vacancies on Mn(2)−Fe(3)−FA may be much higher than those on Mn(1)−Fe(3)−FA. As a result, the capacity of Mn(2)−Fe(3)−FA for elemental mercury capture was generally much better than that of Mn(1)−Fe(3)−FA. Furthermore, Fe^{3+} may have a slight influence on the Hg^0 removal efficiency.[4,11,12,39]

Therefore, the mechanism of elemental mercury captured by Mn(2)−Fe(3)−FA under air may be described as

$$Hg^0_{(g)} + \equiv\bullet \rightarrow \equiv\bullet - Hg^0_{(ad)} \quad (2)$$

$$2\equiv Mn^{IV} + \equiv\bullet - Hg^0_{(ad)} + \equiv O \rightarrow 2\equiv Mn^{III} + Hg^{II}O_{(ad)} \quad (3)$$

$$2\equiv Fe^{III} + \equiv\bullet - Hg^0_{(ad)} + \equiv O \rightarrow 2\equiv Fe^{II} + Hg^{II}O_{(ad)} \quad (4)$$

$$\equiv Mn^{III} + \frac{1}{4}O_2 \rightarrow \equiv Mn^{IV} + \frac{1}{2}\equiv O \quad (5)$$

$$\equiv Fe^{II} + \frac{1}{4}O_2 \rightarrow \equiv Fe^{III} + \frac{1}{2}\equiv O \quad (6)$$

Reactions 5 and 6 explained why elemental mercury capture by Mn(2)−Fe(3)−FA under air was much better than that under N_2. They indicated that the reoxidization of the reduced Mn^{3+} and Fe^{2+} happened. During reoxidization, some cation vacancies may also be recovered.[23] Therefore, when Mn(2)−Fe(3)−FA was exposed in air, its capability of removing mercury was kept stable within 8 h. Furthermore, the oxidized mercury form would be in a solid state below 300 °C,[12,13] which indicated that the formed HgO was very stable at 120 °C, adsorbed on the catalyst, and finally removed from the flue gas.

4. CONCLUSION

The elemental mercury adsorption experiments were carried out with FA and modified FA in a laboratory-scale fixed-bed reactor at 120 °C. The results showed that about 20% of mercury in the flue gas was captured by raw FA at the start of the experiment, but there was no adsorption capacity after 160 min. Impregnation with Mn and Fe increased the mercury removal capacity. The removal efficiencies of Mn(0)−Fe(3)−FA, Mn(1)−Fe(0)−FA, and Mn(1)−Fe(3)−FA were about 38%, 85%, and 82%, respectively. Though the efficiency of Mn(1)−Fe(0)−FA was slightly better than that of Mn(1)−Fe(3)−FA, its efficiency began to decrease after half an hour. The Hg^0 removal efficiency of Mn(1)−Fe(3)−FA was kept basically stable within the experimental time of 8 h. When the amount of impregnated Mn increased, the Hg^0 captured by Mn(2)−Fe(3)−FA stayed around 98%. It was concluded that the cooperation of Mn and Fe had an obvious accelerative effect on Hg^0 removal, and Mn^{4+} may be the main active site. From the performance of mercury capture, Mn(2)−Fe(3)−FA was more likely to be a catalyst, rather than an adsorbent. Furthermore, the TG and XPS results showed that Hg^0 may be physically adsorbed on the cation vacancies incorporated by Mn oxide and ferrites, and then be oxidized to HgO by Mn^{4+} and Fe^{3+}.

In our future work, Mn(2)−Fe(3)−FA will be investigated to capture elemental mercury from the flue gas at a pilot scale, in which the influence of SO_2, CO, NO_x, HCl, NH_3, and H_2O, the separation of FA and HgO, and the catalyst removal stability and recyclability will be further studied.

AUTHOR INFORMATION

Corresponding Author

*Tel.: +86 25 84315517. Fax: +86 25 84315517. E-mail: zq304@mail.njust.edu.cn.

Notes

The authors declare no competing financial interest.

ACKNOWLEDGMENTS

This work was financially supported by the National Natural Science Foundation of China (U1162119 and 51078185), Scientific Research Project of Environmental Protection Department of Jiangsu Province (201112), and Research Fund for the Doctoral Program of Higher Education of China (20113219110009).

REFERENCES

(1) Lee, W.; Bae, G.-N. Removal of Elemental Mercury (Hg(0)) by Nanosized V_2O_5/TiO_2 Catalysts. *Environ. Sci. Technol.* **2009**, *43* (5), 1522−1527.

(2) Yan, N.-Q.; Qu, Z.; Chi, Y.; Qiao, S.-H.; Dod, R. L.; Chang, S.-G.; Miller, C. Enhanced Elemental Mercury Removal from Coal-Fired Flue Gas by Sulfur−Chlorine Compounds. *Environ. Sci. Technol.* **2009**, *43* (14), 5410−5415.

(3) Romero, C. E.; Li, Y.; Bilirgen, H.; Sarunac, N.; Levy, E. K. Modification of boiler operating conditions for mercury emissions reductions in coal-fired utility boilers. *Fuel* **2006**, *85* (2), 204−212.

(4) Presto, A. A.; Granite, E. J. Survey of Catalysts for Oxidation of Mercury in Flue Gas. *Environ. Sci. Technol.* **2006**, *40* (18), 5601−5609.

(5) Krishnan, S. V.; Gullett, B. K.; Jozewicz, W. Sorption of Elemental Mercury by Activated Carbons. *Environ. Sci. Technol.* **1994**, *28* (8), 1506−1512.

(6) Jones, A. P.; Hoffmann, J. W.; Smith, D. N.; Feeley, T. J.; Murphy, J. T. DOE/NETL's Phase II Mercury Control Technology Field Testing Program: Preliminary Economic Analysis of Activated Carbon Injection. *Environ. Sci. Technol.* **2007**, *41* (4), 1365−1371.

(7) Ghorishi, S. B.; Keeney, R. M.; Serre, S. D.; Gullett, B. K.; Jozewicz, W. S. Development of a Cl-Impregnated Activated Carbon for Entrained-Flow Capture of Elemental Mercury. *Environ. Sci. Technol.* **2002**, *36* (20), 4454−4459.

(8) Feng, W.; Borguet, E.; Vidic, R. D. Sulfurization of carbon surface for vapor phase mercury removal − I: Effect of temperature and sulfurization protocol. *Carbon* **2006**, *44* (14), 2990−2997.
(9) Feng, W.; Borguet, E.; Vidic, R. D. Sulfurization of a carbon surface for vapor phase mercury removal − II: Sulfur forms and mercury uptake. *Carbon* **2006**, *44* (14), 2998−3004.
(10) Yang, S. J.; Guo, Y. F.; Yan, N. Q.; Wu, D. Q.; He, H. P.; Qu, Z.; Jia, J. P. Elemental Mercury Capture from Flue Gas by Magnetic Mn-Fe Spinel: Effect of Chemical Heterogeneity. *Ind. Eng. Chem. Res.* **2011**, *50* (16), 9650−9656.
(11) Yang, S. J.; Guo, Y. F.; Yan, N. Q.; Wu, D. Q.; He, H. P.; Xie, J. K.; Qu, Z.; Jia, J. P. Remarkable effect of the incorporation of titanium on the catalytic activity and SO_2 poisoning resistance of magnetic Mn-Fe spinel for elemental mercury capture. *Appl. Catal., B* **2011**, *101* (3−4), 698−708.
(12) Granite, E. J.; Pennline, H. W.; Hargis, R. A. Novel Sorbents for Mercury Removal from Flue Gas. *Ind. Eng. Chem. Res.* **2000**, *39* (4), 1020−1029.
(13) Borderieux, C.; Wu, C. Y.; Bonzongo, J. C.; Powers., K. Control of elemental Mercury Vapor in Combustion Systems Using Fe_2O_3 Nanoparticles. *Aeros. Air Qual. Res.* **2004**, *4* (1), 74−90.
(14) Ahmaruzzaman, M. A review on the utilization of fly ash. *Prog. Energy Combust. Sci.* **2010**, *36* (3), 327−363.
(15) Dunham, G. E.; DeWall, R. A.; Senior, C. L. Fixed-bed studies of the interactions between mercury and coal combustion fly ash. *Fuel Process. Technol.* **2003**, *82* (2−3), 197−213.
(16) Rubel, A. M.; Hower, J. C.; Mardon, S. M.; Zimmerer, M. J. Thermal stability of mercury captured by ash. *Fuel* **2006**, *85* (17−18), 2509−2515.
(17) Wen, X. Y.; Li, C. T.; Fan, X. P.; Gao, H. L.; Zhang, W.; Chen, L.; Zeng, G. M.; Zhao, Y. P. Experimental Study of Gaseous Elemental Mercury Removal with CeO_2/γ-Al_2O_3. *Energy Fuels* **2011**, *25* (7), 2939−2944.
(18) Shen, Z. M.; Ma, J.; Mei, Z. J.; Zhang, J. D. Metal chlorides loaded on activated carbon to capture elemental mercury. *J. Environ. Sci.−Chin.* **2010**, *22* (11), 1814−1819.
(19) Wang, Y. J.; Duan, Y. F. Effect of Manganese Ions on the Structure of $Ca(OH)_2$ and Mercury Adsorption Performance of Mn^{x+}/$Ca(OH)_2$ Composites. *Energy Fuels* **2011**, *25* (4), 1553−1558.
(20) Fan, X.; Li, C.; Zeng, G.; Zhang, X.; Tao, S.; Lu, P.; Tan, Y.; Luo, D. Hg^0 Removal from Simulated Flue Gas over CeO_2/HZSM-5. *Energy Fuels* **2012**, *26* (4), 2082−2089.
(21) Zhang, Z. J.; Wang, Z. L.; Chakoumakos, B. C.; Yin, J. S. Temperature Dependence of Cation Distribution and Oxidation State in Magnetic Mn−Fe Ferrite Nanocrystals. *J. Am. Chem. Soc.* **1998**, *120* (8), 1800−1804.
(22) Gillot, B.; Laarj, M.; Kacim, S. Reactivity towards oxygen and cation distribution of manganese iron spinel $Mn_{3-x}Fe_xO_4$ ($0 \leq x \leq 3$) fine powders studied by thermogravimetry and IR spectroscopy. *J. Mater. Chem.* **1997**, *7* (5), 827−831.
(23) Yang, S. J.; Yan, N. Q.; Guo, Y. F.; Wu, D. Q.; He, H. P.; Qu, Z.; Li, J. F.; Zhou, Q.; Jia, J. P. Gaseous Elemental Mercury Capture from Flue Gas Using Magnetic Nanosized $(Fe_{3-x}Mnx)_{1-\delta}O_4$. *Environ. Sci. Technol.* **2011**, *45* (4), 1540−1546.
(24) Yang, S. J.; Guo, Y. F.; Yan, N. Q.; Qu, Z.; Xie, J. K.; Yang, C.; Jia, J. P. Capture of gaseous elemental mercury from flue gas using a magnetic and sulfur poisoning resistant sorbent Mn/γ-Fe_2O_3 at lower temperatures. *J. Hazard. Mater.* **2011**, *186* (1), 508−515.
(25) Dunham, G. E.; DeWall, R. A.; Senior, C. L. Fixed-bed studies of the interactions between mercury and coal combustion fly ash. *Fuel Process. Technol.* **2003**, *82* (2−3), 197−213.
(26) Guo, P.; Guo, X.; Zheng, C. G. Roles of γ-Fe_2O_3 in fly ash for mercury removal: Results of density functional theory study. *Appl. Surf. Sci.* **2010**, *256* (23), 6991−6996.
(27) Galbreath, K. C.; Zygarlicke, C. J. Mercury transformations in coal combustion flue gas. *Fuel Process. Technol.* **2000**, *65−66* (0), 289−310.
(28) Lu, Y.; Rostam-Abadi, M.; Chang, R.; Richardson, C.; Paradis, J. Characteristics of Fly Ashes from Full-Scale Coal-Fired Power Plants and Their Relationship to Mercury Adsorption. *Energy Fuels* **2007**, *21* (4), 2112−2120.
(29) Li, H. L.; Zhang, J. Y.; Zhao, Y. C.; Wu, C. Y.; Zheng, C. G. Wettability of Fly Ashes from Four Coal-Fired Power Plants in China. *Ind. Eng. Chem. Res.* **2011**, *50* (13), 7763−7771.
(30) Liu, L. Y.; Singh, R.; Xiao, P.; Webley, P. A.; Zhai, Y. C. Zeolite synthesis from waste fly ash and its application in CO_2 capture from flue gas streams. *Adsorp.−J. Int. Adsorp. Soc.* **2011**, *17* (5), 795−800.
(31) Medina, A.; Gamero, P.; Querol, X.; Moreno, N.; De León, B.; Almanza, M.; Vargas, G.; Izquierdo, M.; Font, O. Fly ash from a Mexican mineral coal I: Mineralogical and chemical characterization. *J. Hazard. Mater.* **2010**, *181* (1−3), 82−90.
(32) Pitoniak, E.; Wu, C.-Y.; Mazyck, D. W.; Powers, K. W.; Sigmund, W. Adsorption Enhancement Mechanisms of Silica−Titania Nanocomposites for Elemental Mercury Vapor Removal. *Environ. Sci. Technol.* **2005**, *39* (5), 1269−1274.
(33) Lopez-Anton, M. A.; Yuan, Y.; Perry, R.; Maroto-Valer, M. M. Analysis of mercury species present during coal combustion by thermal desorption. *Fuel* **2010**, *89* (3), 629−634.
(34) Herranz, T.; Rojas, S.; Ojeda, M.; Perez-Alonso, F. J.; Terreros, P.; Pirota, K.; Fierro, J. L. G. Synthesis, Structural Features, and Reactivity of Fe−Mn Mixed Oxides Prepared by Microemulsion. *Chem. Mater.* **2006**, *18* (9), 2364−2375.
(35) Zhang, Y.; Yang, M.; Dou, X.-M.; He, H.; Wang, D.-S. Arsenate Adsorption on an Fe−Ce Bimetal Oxide Adsorbent: Role of Surface Properties. *Environ. Sci. Technol.* **2005**, *39* (18), 7246−7253.
(36) Shen, B.; Liu, T.; Zhao, N.; Yang, X.; Deng, L. Iron-doped Mn-Ce/TiO_2 catalyst for low temperature selective catalytic reduction of NO with NH_3. *J. Environ. Sci.* **2010**, *22* (9), 1447−1454.
(37) Wandelt, K. Photoemission studies of adsorbed oxygen and oxide layers. *Surf. Sci. Rep.* **1982**, *2* (1), 1−121.
(38) Cornell, R. M.; ; Schwertmann, U., *The Iron Oxides: Structure, Properties, Reactions, Occurrences and Uses*; Wiley-VCH: New York, 2003.
(39) Kong, F. H.; Qiu, J. R.; Liu, H.; Zhao, R.; Ai, Z. H. Catalytic oxidation of gas-phase elemental mercury by nano-Fe_2O_3. *J. Environ. Sci.* **2011**, *23* (4), 699−704.